Mem. S.A.It. Vol. 76, 449

Memorie della

X-ray Observations of Hot Gas in Planetary Nebulae

M.A. Guerrero[1], Y.-H. Chu[2], and R.A. Gruendl[2]

[1] Instituto de Astrofísica de Andalucía, CSIC Camino Bajo de Huétor, 50, E-18008 Granada, Spain e-mail: mar@iaa.es
[2] Department of Astronomy, University of Illinois at Urbana-Champaign 1002 West Green Street, Urbana, IL 61801, USA e-mail: chu@astro.uiuc.edu, gruendl@astro.uiuc.edu

Abstract. The formation and shaping of planetary nebulae (PNe) is a complex process that involves the action of multiple agents, including fast stellar winds and collimated outflows. Both fast stellar winds and collimated outflows can produce shock-heated gas that emits diffuse X-rays. Hot gas in PN interiors was hinted by *ROSAT* observations, but unambiguous detections of diffuse X-ray emission were not made until *Chandra* and *XMM-Newton* became available. The unprecedented angular resolution and sensitivity of these new X-ray observations allow us to investigate in detail the physical properties and origin of the hot gas content of PNe and to assess its dynamical effects on the shaping and expansion of PNe. This paper reviews the results from recent X-ray observations of PNe and discusses their implications to our understanding of the formation and evolution of PNe.

Key words. ISM: planetary nebulae: general – star: winds, outflows

1. Introduction

Planetary nebulae (PNe) consist of the stellar material ejected by stars with masses $\leq$ 8–10 $M_\odot$. As such a star evolves off the main sequence, it experiences the first episode of significant mass loss during the red giant phase, and a subsequent episode of major, copious mass loss at the tip of the asymptotic giant branch (AGB). Both the red giant wind and the AGB wind are slow, with terminal velocities of 10–50 km s^{-1}, but the AGB wind is much more intense, with mass loss rates up to a few times $10^{-4} M_\odot$ yr^{-1}, so that it is often called a "superwind". As the stellar envelope is stripped off by this superwind, the hot stellar core is exposed and the stellar UV radiation ionizes the ejected stellar material, causing it to emit in the optical and become a PN.

The central stars of PNe exhibit fast stellar winds with terminal velocities of 1,000–4,000 km s^{-1} (Cerruti-Sola & Perinotto 1985). The dynamic interaction between this fast stellar wind and the previous slow AGB wind has been suggested to give rise to the formation and evolution of a PN (Kwok, Purton, & Fitzgerald 1978). In this interacting-stellar-winds model of PNe, the fast wind emanating from the central star sweeps up the slow AGB wind to form the sharp nebular shell typically observed in PNe.

Send offprint requests to: M.A. Guerrero

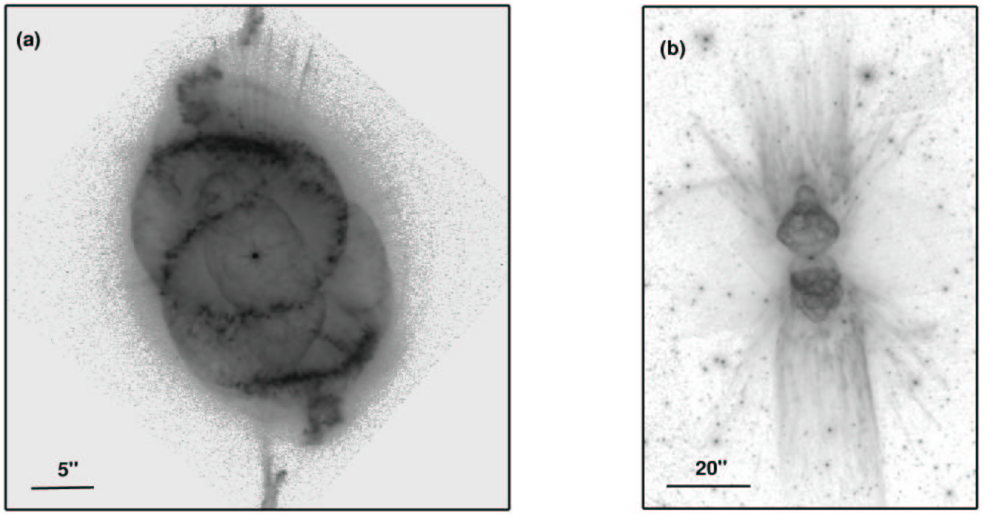

Fig. 1. *HST* WFPC2 narrow-band images of NGC 6543 and Mz 3 illustrating the varied morphology and complex structure of PNe. (a) The [N II] image of NGC 6543 shows an asymmetric inner shell and low-ionization point-symmetric features associated with fast collimated outflows (Miranda & Solf 1992). (b) The [N II] image of Mz 3 reveals a multi-polar morphology associated with fast bipolar outflows along the nebula's axis of symmetry (Guerrero, Chu, & Miranda 2004).

The interacting-stellar-winds model of PNe cannot reproduce the large variety of nebular shapes observed in PNe (Figure 1). In particular, it does not explain collimated outflows and point-symmetric features (e.g., Balick & Frank 2002). Alternatively, point-symmetry could result from the action of multiple collimated outflows at very early phases of the PN evolution, i.e., in the proto-PN stage (Sahai & Trauger 1998). Both fast stellar winds and fast collimated outflows can collide with the ambient medium at velocities greater than 300 km s^{-1} to produce post-shock gas at temperatures $>10^6$ K. X-ray emission from this hot gas provides a window for us to observe how fast stellar winds and/or fast collimated outflows interact with the AGB wind and transfer energy and momentum to the PN envelope. Thus, X-ray observations of PNe can be used to assess the effects of these different agents and to determine their relative importance in the formation and evolution of PNe.

2. Production of Hot Gas in Planetary Nebulae

In the interacting-stellar-winds model of PNe, the physical structure of a PN would consist of (a) a central cavity filled with shocked fast wind at 10^7–10^8 K, (b) a thin, dense shell of swept-up AGB wind at 10^4 K, and (3) an outer envelope of unperturbed expanding AGB wind (Zhekov & Perinotto 1996). The shell of swept-up superwind corresponds to the bright, optically visible PN shell. The surrounding unperturbed superwind can be optically detected as an outer shell attached to the bright main shell. The tenuous hot gas in the central cavity, having a high pressure, drives the expansion of the nebular shell and determines the evolution of the nebula. The hot gas in the central cavity of a PN should emit X-rays, but it is too tenuous to produce appreciable X-ray emission. Dynamic or evaporative mixing of cool nebular material into the hot gas at their interface produces optimal conditions for soft X-ray emission, which will show a limb-brightened morphology within the nebular shell.

Table 1. Chandra and XMM-Newton Detections of Hot Gas in Planetary Nebulae

Planetary Nebula	X-ray Observatory	Count Rate (cnts s^{-1})	Observed Flux (ergs cm^{-2} s^{-1})	Reference
BD+30°3639	Chandra	0.242	5.7×10^{-13}	1
Hen 3-1475	Chandra	0.0015	1.3×10^{-14}	2
Mz 3	Chandra	0.0015	7.5×10^{-15}	3
NGC 2392	XMM-Newton	0.0534	6.0×10^{-14}	4
NGC 3242	XMM-Newton	0.0384	4.0×10^{-14}	5
NGC 6543	Chandra	0.0316	1.0×10^{-13}	6
NGC 7009	XMM-Newton	0.0615	7.2×10^{-14}	7
NGC 7026	XMM-Newton	0.0083	8.8×10^{-15}	8
NGC 7027	Chandra	0.014	3.1×10^{-14}	9

References: (1) Kastner et al. (2000), (2) Sahai et al. (2003), (3) Kastner et al. (2003), (4) Guerrero et al. (2005), (5) Chu et al., in prep., (6) Chu et al. (2001), (7) Guerrero, Gruendl, & Chu (2002), (8) Gruendl et al., in prep., (9) Kastner, Vrtilek, & Soker (2001).

The physical structure of a PN is similar to that of a bubble blown by a massive star (e.g., Weaver et al. 1977) or a young superbubble around an OB association that has not had any supernova explosions. Of all bubbles blown by single massive stars, only two Wolf-Rayet bubbles exhibit detectable diffuse X-ray emission; their X-ray surface brightnesses and plasma temperatures are much lower than expected (e.g., S 308, Chu et al. 2003). Superbubbles around OB associations can be readily detected, but most of them have been energized by supernovae (Chu & Mac Low 1990). The few superbubbles around very young OB associations, such as the Omega Nebula and the Rosette Nebula, show diffuse X-ray emission from $\sim 10^7$ K gas (Townsley et al. 2003), much hotter than those seen in WR bubbles. The vastly different plasma temperatures between WR bubbles and young superbubbles are not well understood. PNe with detected diffuse X-ray emission thus provide an invaluable laboratory to study the dynamical interactions of fast winds with the ambient medium for comparisons with WR bubbles and young superbubbles.

In addition to fast stellar winds, PNe and proto-PNe exhibit fast collimated outflows with velocities up to 1,000 km s^{-1}, e.g., MyCn 18 and Hen 3-1475 (Bobrowsky et al. 1995; Riera et al. 1995; O'Connor et al. 2000). Similar collimated outflows or jets in Herbig-Haro objects and symbiotic stars are known to produce hot X-ray-emitting gas (Pravdo et al. 2001; Kellogg et al. 2001). Therefore, it is expected that outflows in PNe with velocities $\geq$300 km s^{-1} impinging on the AGB wind will also produce bow shocks and X-ray emission. The prolonged action of collimated outflows may bore through the AGB wind and form extended cavities that are filled with shock-heated gas and show diffuse X-rays.

3. X-ray Observations of Planetary Nebulae

X-ray emission from PNe was first detected in *EXOSAT* observations of NGC 1360 (de Korte 1985). Subsequently, archival *Einstein* observations were used to demonstrate X-ray emission from NGC 246, NGC 6853, NGC 7293, and A 33 (Tarafdar & Apparao 1988), and archival *EXOSAT* observations were used to identify X-ray emission from four more PNe, NGC 1535, NGC 4361, NGC 3587, and A 36 (Apparao & Tarafdar 1989). These X-ray sources were interpreted to be photospheric emission from the hot (100,000–200,000 K) central stars.

ROSAT made useful observations of ~60 PNe and provided the first indication of the diffuse X-ray emission expected from hot gas in

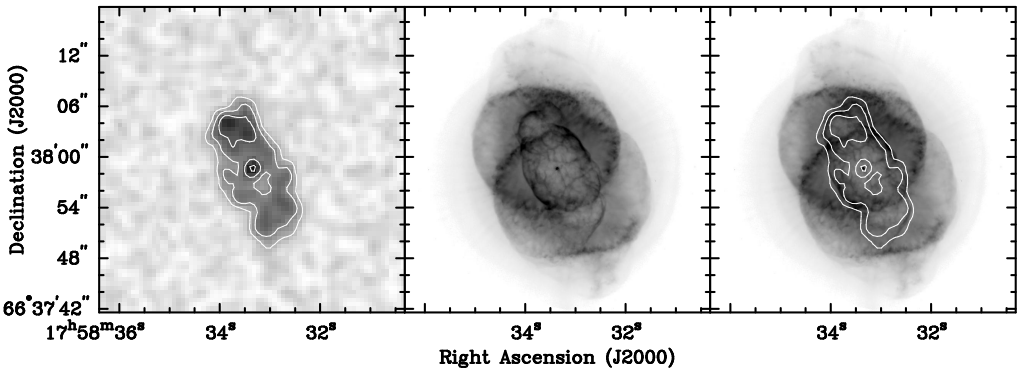

Fig. 2. NGC 6543. *Left*: *Chandra* ACIS-S image in the 0.3–2.0 keV energy band. *Center*: *HST* WFPC2 Hα image. *Right*: Hα image overlaid by X-ray contours. Adapted from Chu et al. (2001).

PN interiors. Of the 13 PNe detected by *ROSAT* (Guerrero, Chu, & Gruendl 2000), three show marginally extended emission: BD+30°3639, NGC 6543, and A30 (Arnaud, Borkowski, & Harrington 1996; Leahy, Kwok, & Yin 2000; Kreysing et al. 1992; Chu, Chang, & Conway 1997). The first two show spectra consistent with plasma emission at a few $\times 10^6$ K, while the last shows a spectrum indicating a cooler ($\sim 5\times 10^5$ K) plasma. These three provide the best candidates for diffuse X-ray emission from PN interiors. Of the 10 unresolved X-ray sources, five show only soft, <0.3 keV, X-rays, two show both a bright soft component and a faint hard (>0.5 keV) component, and the remaining three have spectra too noisy for classification (Guerrero, Chu, & Gruendl 2000). The soft component is consistent with the photospheric emission from the central star, but the hard component may originate from a binary companion or an unresolved volume of hot gas (Leahy et al. 1996; O'Dwyer et al. 2003).

The recently launched *Chandra* and *XMM-Newton* X-ray observatories provide unprecedented sensitivity and angular resolution, which make it possible to detect and resolve the diffuse X-ray emission from hot gas in PNe. To date, observations made with these facilities have unambiguously resolved diffuse X-ray emission from 9 PNe and proto-PNe, as listed in Table 1. Some of these observations have produced exquisite X-ray images and useful spectra, for example, BD+30°3639 (Kastner et al. 2000), NGC 6543 (Chu et al. 2001), and NGC 2392 (Guerrero et al. 2005). Figure 2 illustrates the distribution of diffuse X-ray emission relative to the nebular shell of NGC 6543 (the Cat's Eye Nebula). Comparisons of the X-ray contours and the Hα image of this PN show that the diffuse X-ray emission is bounded by the sharp rim of the central elliptical shell and the two lobes extending along its major axis (Chu et al. 2001).

In general, diffuse X-ray emission is observed to be confined within either the innermost nebular shell for elliptical PNe or the closed lobes for bipolar PNe, consistent with the expected distribution of shocked fast wind in the interacting-stellar-winds model. The only notable exception is the proto-PN Hen 3-1475, for which *Chandra* observations provide the only clear detection of X-ray emission from the bow-shock of a collimated outflow (Sahai et al. 2003).

Recent *XMM-Newton* observations of NGC 2392, the Eskimo Nebula, suggest that both fast stellar winds and collimated outflows may be responsible for its diffuse X-ray emission (Guerrero et al. 2005). NGC 2392 is known for the exceptionally large expansion velocity of its inner shell, $\sim$90 km s^{-1}, and the existence of a fast bipolar outflow with a line-of-sight expansion velocity approaching 200 km s^{-1}. The diffuse X-ray emission from NGC 2392 shows different spatial distributions between the 0.2–0.65 keV and 0.65–2.0 keV

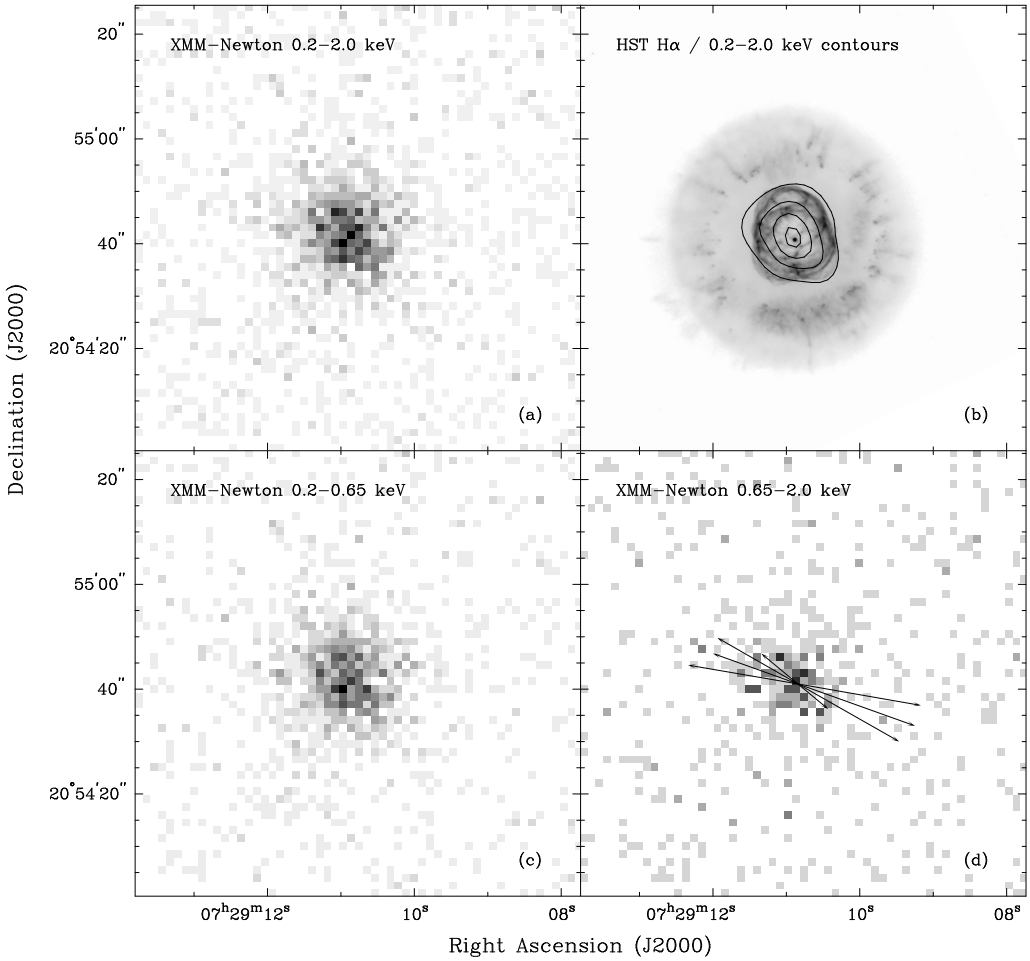

Fig. 3. *XMM-Newton* and *HST* Hα images of the Eskimo Nebula. Panel *(a)* displays the *XMM-Newton* EPIC raw image in the 0.2-2.0 keV band with pixel size 1.″5. Panel *(b)* shows the *HST* Hα image overplotted by the 25%, 50%, 75%, and 95% X-ray contours extracted from the adaptively smoothed 0.2-2.0 keV band image. Panels *(c)* and *(d)* display *XMM-Newton* EPIC raw images in the 0.2-0.65 and 0.65-2.0 keV energy bands, respectively. The pixel size in these images is 1.″5. The arrows in panel *(d)* mark the location of the fast collimated outflow as derived from high-dispersion echelle spectroscopy. Adapted from Guerrero et al. (2005).

bands (Figure 3). The soft X-ray emission is confined within the inner shell as expected from shocked fast wind, while the harder X-ray emission in the 0.65-2.0 keV band is roughly aligned along the fast bipolar outflow, suggesting possible production of hot gas by the interaction of the fast bipolar outflow with nebular material.

The X-ray spectra of four PNe with diffuse X-ray emission are presented in Figure 4. All of these spectra peak at energies <1.0 keV. The spectral shape is dominated by emission lines of N VII, O III, and Ne IX indicative of thin-plasma emission. Spectral fits using a thin-plasma emission model suggest plasma temperatures of 1–3×10^6 K and chemical enrichment of nitrogen and neon. The X-ray lumi-

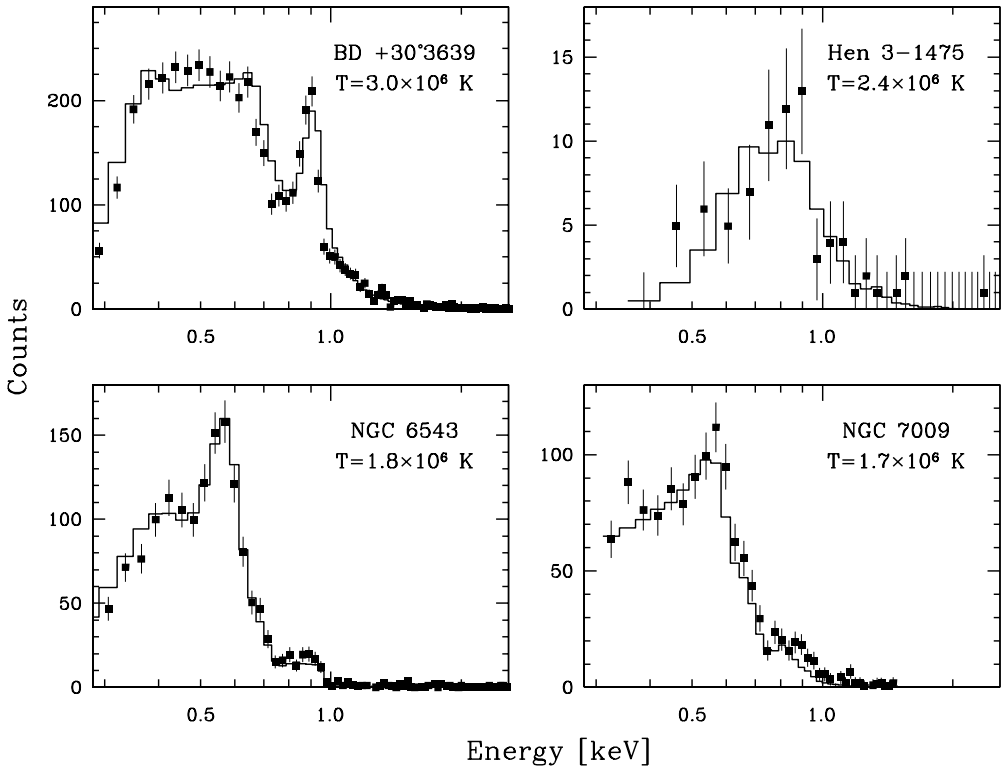

Fig. 4. *Chandra* ACIS-S spectra of BD+30°3639, Hen 3-1475, and NGC 6543, and *XMM-Newton* EPIC/pn spectrum of NGC 7009. The histogram overlaid on each spectrum corresponds to the best-fit model. The temperature of this best-fit model is given in each panel.

nosities of PNe derived from the spectral fits range between 2×10^{31} ergs s^{-1} and 1×10^{33} ergs s^{-1}. The younger PNe (BD+30°3639, Mz 3, and NGC 7027) have higher X-ray luminosities and temperatures than the more evolved PNe (NGC 2392, NGC 6543 and NGC 7009), indicating that the hot gas content of a PN decreases with age. Indeed, *Chandra* and *XMM-Newton* observations of old, evolved PNe have resulted in non-detections.

For PNe with collimated outflows, only the detection of Hen 3-1475 has sufficient counts for spectral analysis; the best-fit plasma temperature is consistent with the post-shock temperature for a ∼400 km s^{-1} shock. PNe with collimated outflows of moderate velocities (<200 km s^{-1}) will have post-shock temperatures too low to produce X-ray emission; indeed, no outflows with moderate velocities have been detected in X-rays.

Chandra's high angular resolution has made it possible to identify the X-ray point source at the central star for Mz 3, NGC 6543, and NGC 7293 (Guerrero et al. 2001; Kastner et al. 2003). Figure 5 shows the X-ray spectra of the central stars of NGC 6543 and NGC 7293. These spectra suggests thin plasma emission at temperatures up to a few $\times10^6$ K and with X-ray luminosities $\sim10^{29}$ ergs s^{-1}. These X-ray point sources may not all have a common origin. In the case of NGC 7293, the Helix Nebula, the central star shows temporal variations in X-rays and in its Hα line profile, suggesting the existence of an unseen dMe companion with coronal activity (Gruendl et al. 2001; Guerrero et al. 2001). As for NGC 6543, the X-ray point source may origi-

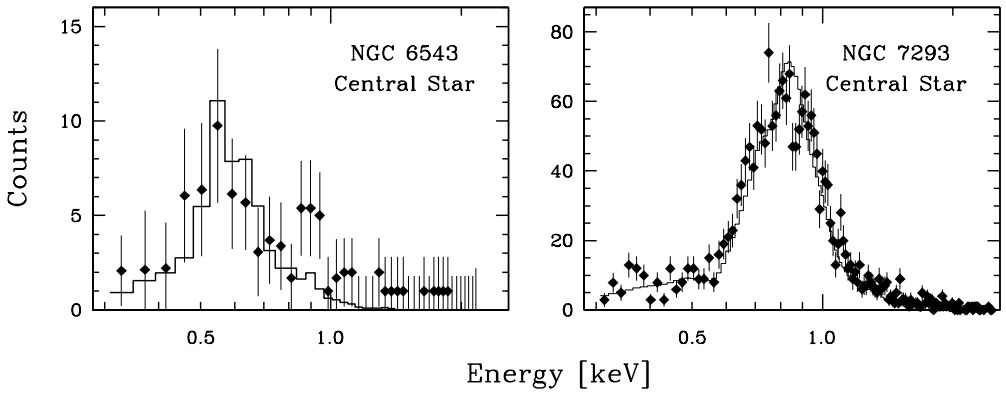

Fig. 5. *Chandra* ACIS-S spectra of the central stars of NGC 6543 and NGC 7293. For comparison, the spectrum of a thin plasma emission model with temperature of 2×10^6 K is overplotted on the X-ray spectrum of NGC 6543. The best-fit model with temperature $\sim7\times10^6$ K is overplotted on the X-ray spectrum of NGC 7293. Adapted from Guerrero et al. (2001).

nate from instability shocks within its fast stellar wind.

4. Conclusions and Future Work

Chandra and *XMM-Newton* observations have made the first unambiguous detections of hot gas in PNe associated with shocked fast winds, collimated outflows, and possibly instability shocks in fast stellar winds. These X-ray observations have provided us with key information to investigate the physical structure of PNe and to assess the roles of fast stellar winds and collimated outflows on the formation and shaping of PNe. It has been shown that young PNe with a sharp shell morphology contain significant amounts of hot gas in their interiors. The distribution of this hot gas agrees with the expectations of wind-blown bubble models, but the physical conditions and X-ray luminosities are discrepant from the model predictions. Comparisons among PNe at different evolutionary stages indicate that the hot gas in a young PN's interior is highly pressurized and drives the nebular expansion, but the hot gas content is drastically reduced over a short time and becomes undetectable. Therefore, the action of the fast stellar wind in the formation and evolution of a PN appears to last for only a small fraction of its nebular lifetime.

The detection of X-ray emission associated with collimated outflows in Hen 3-1475 and possibly NGC 2392 and Mz 3 confirms the effects of fast collimated outflows in the shaping of PNe. Diffuse X-ray emission from PNe with moderate-velocity collimated outflows is not expected, and consequently not detected. NGC 2392 is an interesting case in which both fast wind and outflow may contribute to the production of its hot gas. Deep, high-resolution *Chandra* observations of NGC 2392 are needed to determine the relative importance of stellar wind and outflows in the formation and shaping of its nebular shell.

To date, X-ray observations of PNe have been limited to *Chandra* ACIS or *XMM-Newton* EPIC imaging spectroscopy. The low-dispersion spectra extracted from these observations have allowed us to derive abundance ratios of different elements, but reliable chemical abundances and detailed physical conditions cannot be determined. High-dispersion X-ray spectra are needed. Currently, *Chandra* LETG observations of BD+30°3639 (PI: Kastner) and *XMM-Newton* RGS observations of NGC 6543 (PI: Guerrero) have been scheduled. These high-dispersion grating observations will allow accurate analysis of the hot gas temperature and abundances. The origin and evolution of the hot gas, i.e., the extent of mixing of nebular material into the hot in-

terior, can be diagnosed from its temperature structure and comparisons of its abundances with those of the central star and the optical nebula.

Acknowledgements. M.A.G. is a Fellowship of the Spanish program Ramón y Cajal. He also acknowledges support from the grant AYA 2002-00376 of the Spanish MCyT (cofunded by FEDER funds).

References

Apparao, K. M. V., & Tarafdar, S. P. 1989, ApJ, 344, 826
Arnaud, K., Borkowski, K. J., & Harrington, J. P. 1996, ApJ, 462, L75
Balick, B., & Frank, A. 2002, ARA&A, 40, 439
Bobrowsky, M., Zijlstra, A. A., Grebel, E. K., Tinney, C. G., Te Lintel Hekkert, P., van de Steene, G. C., Likkel, L., & Bedding, T. R. 1995, ApJ, 446, L89
Cerruti-Sola, M. & Perinotto, M. 1985, ApJ, 291, 237
Chu, Y.-H., Chang, T. H., & Conway, G. M. 1997, ApJ, 482, 891
Chu, Y.-H., Guerrero, M. A., Gruendl, R. A., García-Segura, G., & Wendker, H. J. 2003, ApJ, 599, 1189
Chu, Y.-H., Guerrero, M. A., Gruendl, R. A., Williams, R. M., & Kaler, J. B. 2001, ApJ, 553, L69
Chu, Y.-H., & Mac Low, M.-M. 1990, ApJ, 365, 510
de Korte, P. A. J., Claas, J̈J,, Jansen, F. A., & McKechnie, S. P. 1985, AdSpR, 5, 57
Gruendl, R. A., Chu, Y.-H., O'Dwyer, I. J., & Guerrero, M. A. 2001, AJ, 122, 308
Guerrero, M. A., Chu, Y.-H., & Gruendl, R. A. 2000, ApJS, 129, 295
Guerrero, M. A., Chu, Y.-H., Gruendl, R. A., & Meixner, M. 2005, A&A, 430, L69
Guerrero, M. A., Chu, Y.-H., Gruendl, R. A., Williams, R. M., & Kaler, J. B. 2001, ApJ, 553, L55
Guerrero, M. A., Chu, Y.-H., & Miranda, L. F. 2004, AJ, 128, 1694
Guerrero, M. A., Gruendl, R. A., & Chu, Y.-H. 2002, A&A, 387, L1
Kastner, J. H., Balick, B., Blackman, E. G., Frank, A., Soker, N., Vrtílek, S. D., & Li, J. 2003, ApJ, 591, L37
Kastner, J. H., Soker, N., Vrtilek, S. D., & Dgani, R. 2000, ApJ, 545, L57
Kastner, J. H., Vrtilek, S. D., & Soker, N. 2001, ApJ, 550, L189
Kellogg, E., Pedelty, J. A., & Lyon, R. G. 2001, ApJ, 563, L151
Kreysing, H. C., Diesch, C., Zweigle, J., Staubert, R., Grewing, M., & Hasinger, G. 1992, A&A, 264, 623
Kwok, S., Purton, C. R., & Fitzgerald, P. M. 1978, ApJ, 219, L125
Leahy, D. A., Kwok, S., & Yin, D. 2000, ApJ, 540, 442
Leahy, D. A., Zhang, C. Y., Volk, K., & Kwok, S. 1996, ApJ, 466, 352
Miranda, L. F., & Solf, J. 1992, A&A, 260, 397
O'Connor, J. A., Redman, M. P., Holloway, A. J., Bryce, M., López, J. A., & Meaburn, J. 2000, ApJ, 531, 336
O'Dwyer, I. J., Chu, Y.-H., Gruendl, R. A., Guerrero, M. A., & Webbink, R. F. 2003, AJ, 125, 2239
Pravdo, S. H., Feigelson, E. D., Garmire, G., Maeda, Y., Tsuboi, Y., & Bally, J. 2001, Nature, 413, 708
Riera, A., García-Lario, P., Manchado, A., Pottasch, S. R., & Raga, A. C. 1995, A&A, 302, 137
Sahai, R., Kastner, J. H., Frank, A., Morris, M., & Blackman, E. G. 2003, ApJ, 599, L87
Sahai, R., & Trauger, J. T. 1998, AJ, 116, 1357
Tarafdar, S. P., & Apparao, K. MV̇. 1988, ApJ, 327, 342
Townsley, L. K., Feigelson, E. D., Montmerle, T., Broos, P. S., Chu, Y.-H., & Garmire, G. P. 2003, ApJ, 593, 874
Weaver, R., McCray, R., Castor, J., Shapiro, P., & Moore, R. 1977, ApJ, 218, 377
Zhekov, S.A., & Perinotto, M. 1996, A&A, 309, 648